

This document was prepared in conjunction with work accomplished under Contract No. DE-AC09-76SR00001 with the U.S. Department of Energy.

DISCLAIMER

This report was prepared as an account of work sponsored by an agency of the United States Government. Neither the United States Government nor any agency thereof, nor any of their employees, makes any warranty, express or implied, or assumes any legal liability or responsibility for the accuracy, completeness, or usefulness of any information, apparatus, product or process disclosed, or represents that its use would not infringe privately owned rights. Reference herein to any specific commercial product, process or service by trade name, trademark, manufacturer, or otherwise does not necessarily constitute or imply its endorsement, recommendation, or favoring by the United States Government or any agency thereof. The views and opinions of authors expressed herein do not necessarily state or reflect those of the United States Government or any agency thereof.

This report has been reproduced directly from the best available copy.

Available for sale to the public, in paper, from: U.S. Department of Commerce, National Technical Information Service, 5285 Port Royal Road, Springfield, VA 22161, phone: (800) 553-6847, fax: (703) 605-6900, email: orders@ntis.fedworld.gov online ordering: <http://www.ntis.gov/ordering.htm>

Available electronically at <http://www.doe.gov/bridge>

Available for a processing fee to U.S. Department of Energy and its contractors, in paper, from: U.S. Department of Energy, Office of Scientific and Technical Information, P.O. Box 62, Oak Ridge, TN 37831-0062, phone: (865) 576-8401, fax: (865) 576-5728, email: reports@adonis.osti.gov

ACC. NO. 142493

DISTRIBUTION:

R. Maher, SRP
P. M. Pitts
R. G. Baxter (2)
S. Mirshak, SRL
D. L. McIntosh
J. A. Kelley
J. R. Wiley
G. G. Wicks
P. H. Chismar
A. T. Osborne

M. D. Boersma (4)
H. L. Hull
W. M. Taylor
T. A. Willis
G. W. Becker
M. J. Plodinec
J. F. Ortaldo
P. D. d'Entremont
TIS File (2)

June 5, 1980

M E M O R A N D U M

TIS FILE
RECORD COPY

TO: J. K. OKESON

FROM: K. R. ROUTT

KRR

THEORETICAL PREDICTIONS OF MELTING RATE
IN A DRY-FED CYLINDRICAL GLASS MELTER

INTRODUCTION AND SUMMARY

Many tests involving the feeding of solid materials to joule-heated melters have been conducted both at PNL and SRL. In general, there has been considerable variation in melter design and performance, making it difficult to evaluate and predict the melting rate of any given melter.

The question of melt rate is approached herein from a theoretical basis, involving a force, mass, and energy balance on a feedpile floating on the melt surface. A melt rate equation is developed which is then applied to existing data from both PNL and SRL melters. In general, the theory predicts the performance of each melter quite well, thus providing a unified approach to future melter design and evaluation.

The theory suggests criteria for selecting melt depth, free-board above the melt line, and the run time required to determine accurate melt rate. A factor of 2-4 increase in melt rate of most existing melters is predicted if the feedpile can be distributed such that most of the melt surface is covered. An additional factor of 2-3 increase in melt rate is predicted if the wall and lid temperature above the melt line can be increased from 600-800°C to 1000°C. The melt rate equation is expressed in graphical form (Fig. 3) as a function of wall temperature above the meltline and glass boundary layer thickness. This curve should provide a simple means of predicting melt rate for future melters, e.g. 675-G melter.

The basic theory and inferences developed here are applicable to in-can melters. A similar approach will be applied to slurry-fed melters when more phenomenological information is available. The presence of foam is not accounted for in this analysis and is probably the largest single limitation.

Melt Rate for Solid Feed

Consider a cylindrical, joule-heated melter in which solid, incoming feed piles up on the glass surface with an angle of repose θ (Fig. 1). If the density of the feed is ρ_f , then the downward gravitational force F_d acting on the feed material above the meltline is

$$F_d = 1/3\pi R_f^2 \times R_f \tan\theta \times \rho_f g / g_0 \quad (1-1)$$

where

R_f = radius of the feed pile [ft]

g = local gravity [ft/sec²]

g_0 = standard gravitational constant [32.14 lb_m-ft/lb_f-sec²].

This must be balanced by an upward buoyant force F_u , which by Archimedes principle, is equal to the weight of the displaced fluid. Thus, if the density of the molten glass is ρ_g , and the geometry of the displaced glass is also conical, then

$$F_d = F_u \quad (1-2)$$

$$\frac{g\pi R_f^3 \rho_f \tan\theta}{3g_0} = \frac{g\pi R_f^2 d_{fb} \rho_g}{3g_0} \quad (1-3)$$

or

$$d_{fb} = \frac{R_f \rho_f \tan\theta}{\rho_g} \quad (1-4)$$

where

d_{fb} = depth of the feed pile below the meltline [ft].

The surface area available for heat transfer from the glass to the feed is the lateral surface area of the submerged cone A_b , where

$$A_b = \pi R_f^2 \sqrt{R_f^2 + d_{fb}^2} \quad (1-5)$$

Using (1-4) in (1-5) gives

$$A_b = \pi R_f^2 \left[1 + \frac{\rho_f^2 \tan^2 \theta}{\rho_g^2} \right]^{1/2} \quad (1-6)$$

The maximum depth of the submerged feed pile occurs when the radius of the feedpile equals the radius of the melter R_m . To prevent unmelted feed material from being swept into the throat, it is suggested that the melter be designed such that

$$d_t > d_{fb} \quad \left| \quad \max = \frac{R_m \rho_f \tan \theta}{\rho_g} \quad (1-7)$$

where

d_t = distance from the melt line to the top of the throat [ft].

For frit 211 + TDS waste, (1-7) gives*

$$d_t > 0.457 R_m \quad (1-8)$$

The height of the feed pile above the melt surface is (Fig. 1)

$$h_{fa} = R_f \tan \theta \quad (1-9)$$

If the feed pile extends to the melter sidewall, then the desired freeboard above the meltline H_{fb} (Fig. 1) is

$$H_{fb} \geq R_m \tan \theta \quad (1-10)$$

* $\rho_f = 1.28$ g/cc, $\rho_g = 2.8$ g/cc, $\theta \approx 45^\circ$

A mass balance for the feedpile requires that

$$\frac{d}{dt} (\rho_f V_f) = w_i - w_o \quad (1-11)$$

where

$$\begin{aligned} t &= \text{time [hrs]}, \\ V_f &= \text{volume of the feedpile [ft]}, \\ w_i &= \text{feedrate [lbs/hr]}, \text{ and} \\ w_o &= \text{meltrate [lbs/hr]}. \end{aligned}$$

The volume of the feedpile is given by

$$V_f = \frac{1}{3} \pi R_f^2 (h_{fa} + d_{fb}) \quad (1-12)$$

Using (1-9) and (1-4) in (1-12), gives

$$\begin{aligned} V_f &= \frac{1}{3} \pi R_f^2 \left[R_f \tan \theta + \frac{R_f \rho_f \tan \theta}{\rho_g} \right] \\ &= \frac{1}{3} \pi R_f^3 \tan \theta \left[1 + \frac{\rho_f}{\rho_g} \right] \end{aligned} \quad (1-13)$$

Thus, (1-11) becomes

$$\boxed{\frac{\pi \rho_f R_f^2 (\rho_f + \rho_g) \tan \theta}{\rho_g} \frac{dR_f}{dt} = w_i - w_o} \quad (1-14)$$

If w_i and w_o are time independent, integration of (1-14) yields

$$\frac{\pi \rho_f (\rho_f + \rho_g) \tan \theta}{\rho_g} \int_{R_f(t_1)}^{R_f(t_2)} R_f^2 dR_f = \int_{t_1}^{t_2} (w_i - w_o) dt \quad (1-15)$$

or

$$R_f^3(t_2) - R_f^3(t_1) = \frac{3\rho_g(w_i - w_o)(t_2 - t_1)}{\pi\rho_f(\rho_f + \rho_g)\tan\theta} \quad (1-16)$$

which predicts the radius of the melt pile as a function of time.

Alternatively, (1-16) can be used to predict the height of the feedpile as a function of time by using (1-9), that is

$$h_{fa}^3(t_2) - h_{fa}^3(t_1) = \frac{3\rho_g(w_i - w_o)(t_2 - t_1)\tan^2\theta}{\pi\rho_f(\rho_f + \rho_g)} \quad (1-17)$$

Now suppose that feed to an idling melter begins when

$$\begin{aligned} t_1 &= 0 \\ h_{fa}(t_1) &= 0 \end{aligned} \quad (1-18)$$

then (1-17) becomes

$$h_{fa}(t) = \left[\frac{3\rho_g(w_i - w_o)t \tan^2\theta}{\pi\rho_f(\rho_f + \rho_g)} \right]^{1/3} \quad (1-19)$$

and the rate of change in height of the feedpile is

$$\frac{dh_{fa}(t)}{dt} = 1/3 \left[\frac{3\rho_g(w_i - w_o)\tan^2\theta}{\pi\rho_f(\rho_f + \rho_g)} \right]^{1/3} \times t^{-2/3} \quad (1-20)$$

Equation (1-19) can be used to estimate the accuracy of melt rate measurements as will now be demonstrated for the small cylindrical melter at TNX. Postulating an error in feedrate w_i such that the melt rate w_o is given by

$$w_o = \epsilon w_i, \quad 0 \leq \epsilon < 1 \quad (1-21)$$

and assuming that the maximum permissible height of the feedpile above the meltline is the available freeboard H_{fb} (6" for this melter) results in the curves of h_{fa} versus time shown in Fig. 2.

NO. 340R-20 DIETZGEN GRAPH PAPER
DIETZGEN CORPORATION
MADE IN U.S.A.
20 X 20 PER INCH

h_{fa} (inches)

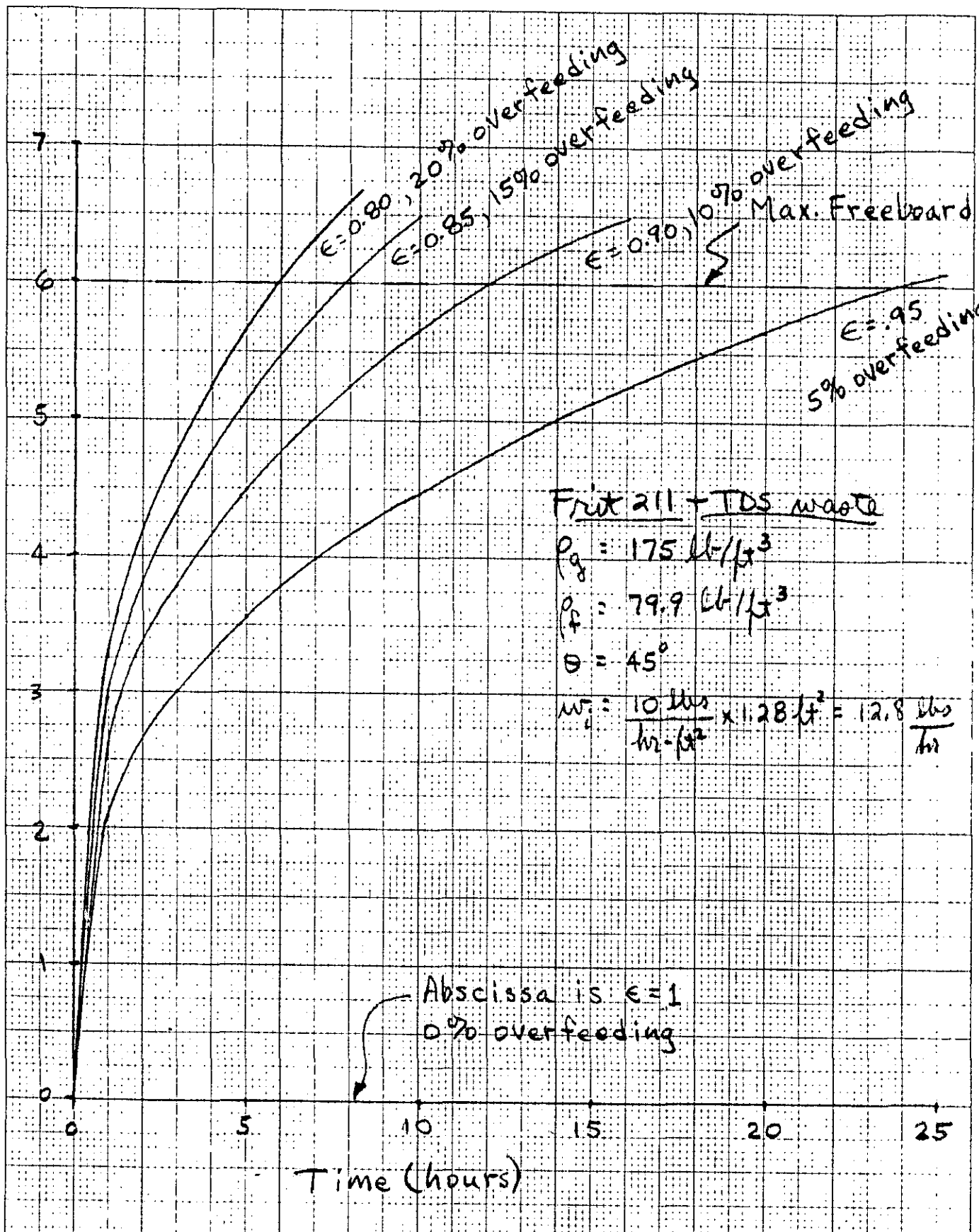


Fig. 2 - Effect of Overfeeding on Feedpile Height versus Time for the Small Cylindrical Melter at TNX

Note that if the feedrate exceeds the meltrate by only 5%, 23.8 hours are required for the feedpile to reach its maximum permissible height. Furthermore, overfeeding by 20% requires 5.95 hours for the feedpile to reach the same height.

Equation (1-20) indicates that the rate of change in height of the feedpile is proportional to $t^{-2/3}$. Hence, once the feedpile is established it becomes increasingly more difficult to detect its growth or recession as time progresses.

In general, a melter is usually initially overfed to establish a cap of some desired height in order to reduce radiant losses from the melt. In the above example, if the melter is overfed to establish the cap at $h_{fa} = 4$ inches, and then the feed rate is reduced in an attempt to reach a steady state feed rate, a 5% error in overfeeding will require 7 hours to increase h_{fa} from 4 to 5 inches; a 10% error will require 3.4 hours, etc. (Fig. 2). Considerable care in the interpretation of melt rate data appears warranted.

An energy balance for the feedpile requires that

$$\rho_f c_{pf} V_f \frac{d\bar{T}_f}{dt} = Q_c + Q_r + Q_i \quad (1-22)$$

where

c_{pf} = specific heat of the feed [BTU/hr -°F],

\bar{T}_f = average temperature of the feedpile [°F],

Q_c = heat conducted into the feedpile from the glass [BTU/hr],

Q_r = radiant heat transmitted to the feedpile from above the meltline [BTU/hr],

Q_i = net internal energy added to the feedpile by the addition of fresh feed and the melting of existing feed [BTU/hr].

Using Fourier's law of heat conduction and (1-6) gives (Fig. 1)

$$Q_c \approx k_g \pi R_f^2 \left[1 + \frac{\rho_f^2 \tan^2 \theta}{\rho_g^2} \right]^{1/2} \frac{(T_g - T_m)}{\delta_t} \quad (1-23)$$

where

k_g = thermal conductivity of the glass [BTU/hr-ft-°F],

δ_t = thickness of the boundary layer in the glass beneath the feedpile [ft],

T_g = bulk glass temperature [°F],

T_m = melt temperature of the feed [°F].

Radiant energy transmission to that portion of the feedpile above the melt surface is given by Stefan-Boltzmann's law

$$Q_r = \sigma [A_w \epsilon_w f_w T_w^4 - A_a \epsilon_a f_a T_a^4] \quad (1-24)$$

where

σ = Stefan-Boltzmann constant

$$= 0.1713 \times 10^{-8} \text{ BTU/hr-ft}^2 \text{-}^{\circ}\text{R}^4$$

A_w = melter wall (and lid) area above the melt line [ft²],

ϵ_w = emissivity of the wall (assume 1.0),

f_w = view factor for radiant transmission from wall the feedpile,

T_w = wall temperature [°R],

A_a = lateral surface area of the feedpile above the meltline [ft²],

ϵ_a = emissivity of the feedpile (assume 1.0),

f_a = view factor for radiant transmission from the feedpile to the wall,

T_a = surface temperature of the feedpile [°R].

If the melter lid is well insulated so that the lid temperature T_l is approximately equal to the wall temperature T_w , then there is no radiant transmission from one melter wall to another, and the lid acts like a plane source directly above the feedpile, radiating to it.

Thus,

$$A_w \epsilon_w f_w \approx A_a \epsilon_a f_a \approx A_a \quad (1-25)$$

and (1-24) is approximately

$$Q_r = \sigma A_a [T_w^4 - T_a^4] \quad (1-26)$$

The area of the feedpile above the melt surface is

$$A_a = \pi R_f \sqrt{R_f^2 + h_{fa}^2} \quad (1-27)$$

Using (1-9) in (1-27) gives

$$\begin{aligned} A_a &= \pi R_f^2 \sqrt{1 + \tan^2 \theta} \\ &= \pi R_f^2 \sec \theta \\ &= \frac{\pi R_f^2}{\cos \theta} \end{aligned} \quad (1-28)$$

Thus, (1-26) becomes

$$Q_r = \frac{\sigma \pi R_f^2 [T_w^4 - T_a^4]}{\cos \theta} \quad (1-29)$$

The net internal energy transfer to the feedpile is (Fig. 1)

$$Q_i = w_i c_{pi} T_i - w_o c_{po} T_m \quad (1-30)$$

where

c_{pi} = specific heat of the incoming feed [BTU/lb-°F],

T_i = temperature of the incoming feed [°F],

c_{po} = specific heat of the feed as it leaves the feedpile and melts into the glass (BTU/lb-°F),

T_m = temperature of the feed as it melts into the glass [°F].

For continuous feeding of the melter, let

$$T_a = T_i$$

$$\bar{T} \approx \frac{T_m + T_a}{2} = \frac{T_m + T_i}{2} \quad (1-31)$$

The energy balance for the feedpile (1-22) can now be written as (using 1-13)

$$\begin{aligned} & \frac{\rho_f c_{pf} \pi R_f^3 \tan \theta (\rho_g + \rho_f)}{6 \rho_g} \frac{d(T_m + T_i)}{dt} = \\ & k_g \pi R_f^2 \left[1 + \frac{\rho_f^2 \tan^2 \theta}{\rho_g^2} \right]^{1/2} \frac{(T_g - T_m)}{\delta_t} + \frac{\sigma \pi R_f^2}{\cos \theta} [T_w^4 - T_i^4] + \\ & \left[\frac{\pi \rho_f R_f^2 (\rho_f + \rho_g) \tan \theta}{\rho_g} \frac{dR_f}{dt} + w_o \right] c_{pi} T_i - w_o c_{po} T_m \quad (1-32) \end{aligned}$$

where the conservation of mass equation (1-14) has been used to express w_i . Equation (1-32) is a general differential equation for the prediction of meltrate w_o versus time.*

The steady state melt rate occurs when

$$\frac{d}{dt} (T_m + T_i) = \frac{dR_f}{dt} = 0 \quad (1-33)$$

* Assuming that T_m , T_i , T_g , and T_w are held constant in time, (1-33) can be easily integrated to predict meltrate as a function of R_f if desired. Ideally, R_f should be made equal to R_m when the melter is being fed.

in which case (1-32) yields

$$w_o = \frac{k_g \pi R_f^2 \left[1 + \frac{\rho_f^2 \tan^2 \theta}{\rho_g^2} \right]^{1/2} \frac{(T_g - T_m)}{\delta_t} + \frac{\sigma \pi R_f^2 [T_w^4 - T_i^4]}{\cos \theta}}{c_{po} T_m - c_{pi} T_i} \quad (1-34)$$

It is convenient when comparing the melt rate of different melters to express (1-34) in terms of a mass flux ϕ [lb/hr-ft²], where

$$\phi = \frac{w_o}{\pi R_m^2} = \frac{k_g \left[1 + \frac{\rho_f^2 \tan^2 \theta}{\rho_g^2} \right]^{1/2} \frac{(T_g - T_m)}{\delta_t} + \frac{\sigma [T_w^4 - T_i^4]}{\cos \theta}}{c_{po} T_m - c_{pi} T_i} \quad (1-35)$$

where it is assumed that the feedpile is maintained at its maximum size, i.e.,

$$R_f = R_m \quad (1-36)$$

Using the data in Table 1, melt rate fluxes have been computed and are shown in Figure 3. At low wall temperatures ($T_w < 400^\circ\text{C}$).

Table 1 - Typical Data for Defense Waste Glass

$$k_g = 2.55 \text{ BTU/hr-ft } ^\circ\text{F (from TDS - frit 21 + composite)}$$

$$\rho_f = 79.9 \text{ lbs/ft}^3 \text{ (frit 211 + TDS waste)*}$$

$$\rho_g = 175 \text{ lbs/ft}^3 \text{ (frit 211 + TDS waste)*}$$

$$\theta \approx 45^\circ \text{ (estimated)}$$

$$\delta_t = 1\text{-}4 \text{ inches (computer simulation and physical model studies)}$$

$$c_{po} = .333 \text{ BTU/lb-}^\circ\text{F (from TDS - frit 21 + composite)}$$

$$c_{pi} = .186 \text{ BTU/lb-}^\circ\text{F (from TDS - frit 21 + composite)}$$

(Table 1 - Continued...)

$$T_g = 1150^\circ\text{C}$$

$$T_m = 800\text{-}850^\circ\text{C} \text{ (computer simulation)}$$

$$T_i = 25^\circ\text{C} \text{ (higher if melter is coupled to a calciner)}$$

$$T_w = 200\text{-}1000^\circ\text{C}$$

*

Data courtesy of M. J. Plodinec

the melt rate is primarily determined by conduction through the melt to the feedpile. Above about 800°C , radiant heat transfer from the walls (lid) becomes the dominant source of energy transfer to the feedpile (Fig. 4). Indeed, for $T_w \geq 1000^\circ\text{C}$, heat transfer from the melt to the feedpile (for $3 < \delta_t < 4$ inches) is relatively small, and the mass flux ϕ of a joule-heated melter should be comparable to that of an in-can melter. Furthermore, equation (1-34) shows that the melt rate w_0 is directly proportional to the square of the radius of the feedpile R_F .

This suggests the following additional melter design criteria:

- High thermal conductivity material should be used above the melter freeboard H_{fb} to enhance the transfer of joule heat up the sidewalls to the region above the melt line. Possible candidate materials such as SiC brick* or Inconel 690 plate are suggested. Top entering Inconel 690 electrodes would also enhance radiant heat transfer to the feedpile.
- A highly insulated melter lid is desirable.
- Some means of distributing the feedpile over the melt surface should give a substantial boost in meltrate.
- Lid heaters should boost the melt rate tremendously, provided that foam formation does not become the limiting mechanism.

*

See for example Carbofrax A, D and M made by the Carborundum Company.

Table 2 compares theoretical mass fluxes ϕ with observed data from several sources. In every case, the maximum theoretical flux ϕ (column 12), has been multiplied by the actual fractional area of the melt surface occupied by the feedpile (column 10) to obtain the theoretical value of ϕ (column 11) for a given melter. This should be compared with the experimental values given in columns 6 and 7. The data strongly suggest that failure to distribute the feed over the melt surface is severely limiting melter throughput. This is particularly emphasized by comparing the mass flux of the small cylindrical melter at TNX with hot walls (1000-1050°C) and poor feed distribution (15-27% coverage) to the mass flux of the DLF melter with cold walls (300°C) and excellent feed distribution (~100% coverage). Lid heat plus full coverage of the melt surface should give the melter performance shown in Fig. 3.*

Unfortunately, in many cases, direct comparison of melter performance with the theory is difficult because of insufficient data. Estimated data values are indicated in Table 2 by question marks. In general though, the theory and available data agree quite well, and it appears that current joule-heated melter designs could be significantly improved.

* *Provided foam formation is not limiting.*

DIETZGEN CORPORATION
MADE IN U.S.A.

NO. 34DR-20 DIETZGEN GRAPH PAPER
20 X 20 PER INCH

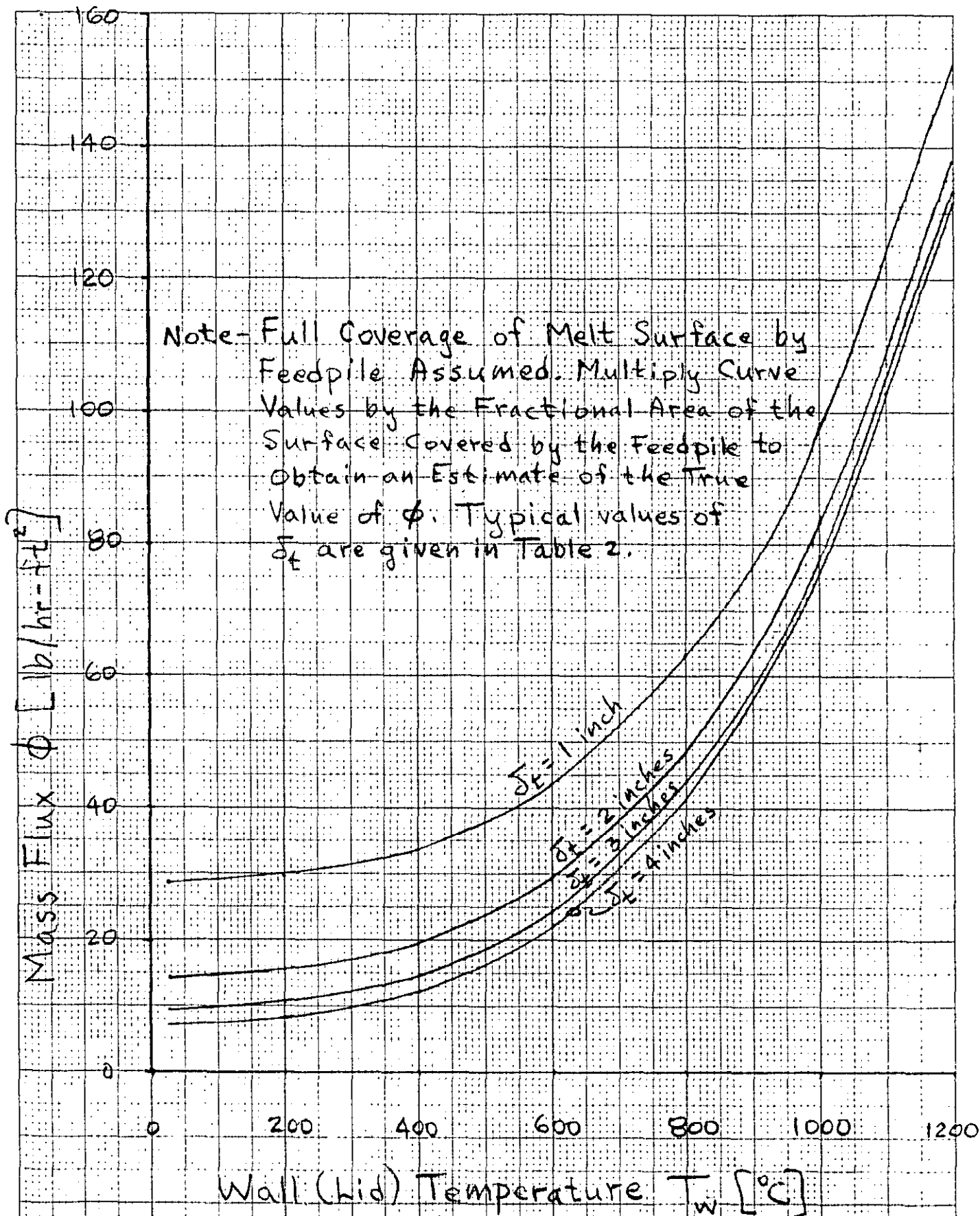


Figure 3 - Melt Rate versus Glass Boundary Layer Thickness δ_t and Wall Temperature T_w

DIETZGEN CORPORATION
MADE IN U.S.A.

NO. 340R-20 DIETZGEN GRAPH PAPER
1 20 X 20 PER INCH

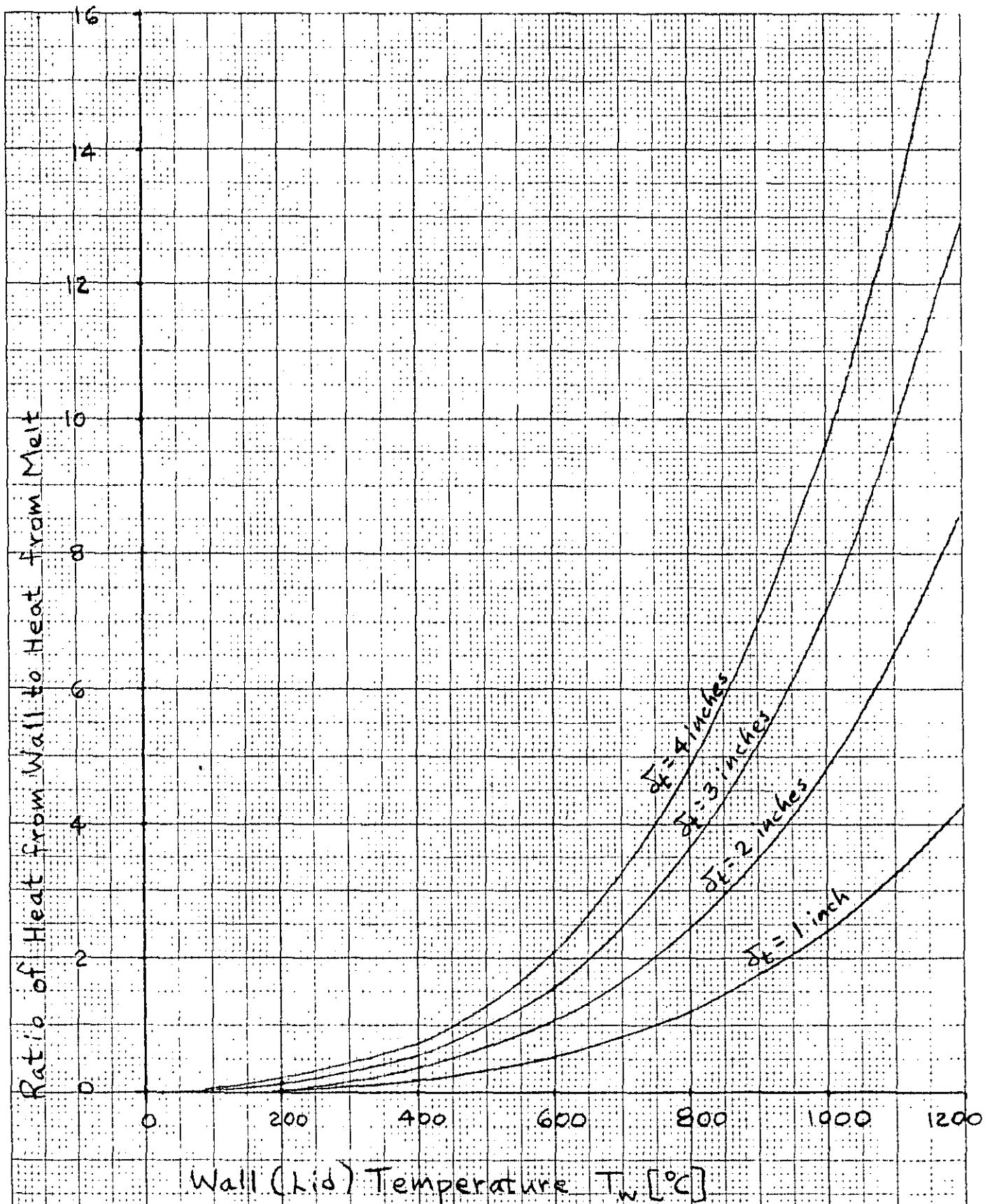


Figure 4 - Effect of Radiant Heat as a Function of Boundary Layer Thickness δ_t

TABLE 2 - COMPARISON OF THEORETICAL AND EXPERIMENTAL MELT RATES

Equipment	Reference	T _g (°C)	T _w (°C)	δ _t (inches)	Measured Nominal φ (lb/hr-ft ²)	Measured Max. φ (lb/hr-ft ²)	Surface Area (ft ²)	Glass	% of Surface Covered by Feedpile	Theoretical φ from Fig. 3 (lb/hr-ft ²)	Max. Theoretical φ from Fig. 3 (lb/hr-ft ²)
2D Computer Simulation of 675G Melter	1	1150	----	1-1.5	15-20*	----	12.6	Frit 21 + composite	100	----	----
3D Physical Model of 675G Melter	2	1150	----	3-4	>7.3*	----	3.14	Frit 21 + composite	100	----	----
CTD Melter at 773-A	3	1150	~700	1-2.5?	----	4.74	.167	Frit 21 + composite	25	8.8-13.3	35-53
	3	1150	~700	1-2.5?	----	7.90	.167	Frit 411 + Simulated Waste	25		
	4	1150	~700	1-2.5?	----	14.1	.167	Frit 211 + high Fe	25		
Small Rectan- gular Melter at TNX	5	1170	500+	~1.5	14.2	----	.901	Frit 411 + composite	33	10.0+	30+
	5	1170	500+	~1.5	15.0	----	.901	Frit 211 + TDS	<33		
Small Cylin- drical Melter at TNX	6	1130- 1180	1000- 1050	4-5	----	13-17	1.28	Frit 211 + TDS	15-27	12.8-23.8	85-88
	6	1130- 1180	600- 800?	4-5	----	4.9-6.5	1.28	Frit 211 + TDS	15-27	3.0-11.3	20-42

TABLE 2.- COMPARISON OF THEORETICAL AND EXPERIMENTAL MELT RATES (Cont'd)

Equipment	Reference	T_g (°C)	T_w (°C)	δt (inches)	Measured Nominal ϕ (lb/hr-ft ²)	Measured Max. ϕ (lb/hr-ft ²)	Surface Area (ft ²)	Glass	% of Surface Covered by Feedpile	Theoretical ϕ from Fig. 3 (lb/hr-ft ²)	Max. Theoretical ϕ from Fig. 3 (lb/hr-ft ²)
CFCM Melter at PNL											
- CFCM5	7-9	1100- 1250	650- 750	3-5	10.3-11.1	12.9	8.56	Frit 411 + composite			
- CFCM6	10,11	1150- 1230	650- 700?	3-5?	16.7	20.6	8.56	Frit 411 + TDS, Frit 211 + TDS	~37	9.6-13.3	26-36
- CFCM7	11,12	1260- 1340	650- 700?	3-5?	14.6	18.0	8.56	Frit 211 + TDS			
- Sodium Silicate	13	1050- 1070	650- 700?	3-5?	12.8-15.4	----	8.56	Frit 211-SS + TDS			
DLF Melter at PNL	14	1290	300	4.3	12.7-20.0	20.0	11.33	Frit + Han- ford Waste	~100	>9.0	>9.0
	15	1179	500- 700?	----	8.09	9.93	11.33	Batch 411 + composite			
	15	1213	500- 700?	----	----	17.7	11.33	Frit 411 + composite			
	16	1210	500- 700?	9?	7.65	10.3	11.33	Frit 211 + TDS	~49	7.8-15.2	16-31
	17	1190	500- 700?	4	----	17.7	11.33	Frit 211 + TDS			

* Calculated values

REFERENCES

1. B. E. Murphree, Personal communication.
2. K. R. Routt, Unpublished data from physical model studies of the 675-G melter at TNX.
3. M. J. Plodinec, *Vitrification of Savannah River Plant Radioactive Waste - Process Development Studies*, DP-MS-79-42, October 10-12, 1979.
4. M. J. Plodinec, Personal communication.
5. B. E. Murphree, *Small Scale Melter Performance*, DPST-79-542, October 30, 1979.
6. M. J. Plodinec and K. R. Routt, *Effects of Electrode Firing Pattern and Lid Heaters on Glass Melting*, DPST-80-318, March 28, 1980.
7. H. L. Hull, *Trip Report, Battelle-Pacific Northwest Laboratories, Spray Calcining -- Continuous Melting -- 10 Day Test*, September 19-29, 1978, DPST-78-541, October 16, 1978.
8. W. J. Bjorklund, Personal communication.
9. R. D. Dierks, *The Performance of the Calcine-Fed Ceramic Melter During Prolonged Normal Operating Conditions - Experiment CFCM-5*, PNL-2905, January, 1979.
10. H. L. Hull, *Trip Report, Battelle-Pacific Northwest Laboratories, Spray Calcining -- Continuous Melting -- 10 Day Test*, April 17-28, 1979, DPST-79-394, May 30, 1979.
11. J. L. McElroy et. al., *Quarterly Progress Report - Research and Development Activities - High Level Waste Immobilization Program: April - June, 1979*, PNL-3050-2, December, 1979.
12. H. L. Hull, *Trip Report, Battelle-Pacific Northwest Laboratories, Spray Calcining -- Continuous Melting -- 25 Day Test*, June 4-30, 1979, DPST-79-446, July 23, 1979.
13. H. L. Hull, *Trip Report, Battelle-Pacific Northwest Laboratories, Spray Calcining -- Continuous Melting -- 5 Day Test*, November 5-9, 1979, DPST-79-593, December 4, 1979.
14. C. C. Chapman et. al., *Vitrification of Hanford Wastes in a Joule-Heated Ceramic Melter and Evaluation of Resultant Canisterized Product*, PNL-2904, August, 1979.
15. H. L. Hull, *Trip and Test Report, Battelle-Pacific Northwest Laboratories, Continuous Electric Melting Tests, December 10-15, 1978 and January 10, 1979*, DPST-79-233, January 25, 1979.

REFERENCES (Cont'd.)

16. H. L. Hull, *Trip Report, Battelle-Pacific Northwest Laboratories, Continuous Melting and Spray Calcining -- In-Can Melting Tests, July 23 - August 3, 1979, DPST-79-492, September 19, 1979.*
17. H. L. Hull, *Trip Report, Battelle-Pacific Northwest Laboratories, Continuous Electric Melting Test, October 1-4, 1979, DPST-79-550, October 30, 1979.*